AMERICAN SOCIETY FOR MICROBIOLOGY | Applied and Environmental Microbiology®

ENVIRONMENTAL MICROBIOLOGY

The Lonely Guy (LOG) Homologue SiRe_0427 from the Thermophilic Archaeon *Sulfolobus islandicus* REY15A Is a Phosphoribohydrolase Representing a Novel Group

Joseph Badys Mayaka,[a] Qihong Huang,[a] Yuanxi Xiao,[a] Qing Zhong,[a] Jinfeng Ni,[a] Yulong Shen[a]

[a]State Key Laboratory of Microbial Technology, Microbial Technology Institute, Shandong University, Qingdao, People's Republic of China

ABSTRACT Lonely Guy (LOG) proteins are important enzymes in cellular organisms, which catalyze the final step in the production of biologically active cytokinins via dephosphoribosylation. LOG proteins are vital enzymes in plants for the activation of cytokinin precursors, which is crucial for plant growth and development. In fungi and bacteria, LOGs are implicated in pathogenic or nonpathogenic interactions with their plant hosts. However, LOGs have also been identified in the human pathogen *Mycobacterium tuberculosis*, and the accumulation of cytokinin-degraded products, aldehydes, within bacterial cells is lethal to the bacterium in the presence of nitric oxide, suggesting diverse roles of LOGs in various species. In this study, we conducted biochemical and genetic analysis of a LOG homologue, SiRe_0427, from the hyperthermophilic archaeon *Sulfolobus islandicus* REY15A. The protein possessed the LOG motif GGGxGTxxE and exhibited phosphoribohydrolase activity on adenosine-5-monophosphate (AMP), similar to LOGs from eukaryotes and bacteria. Alanine mutants at either catalytic residues or substrate binding sites lost their activity, resembling other known LOGs. SiRe_0427 is probably a homotetramer, as revealed by size exclusion chromatography and chemical cross-linking. We found that the gene encoding SiRe_0427 could be knocked out; however, the Δ*sire_0427* strain exhibited no apparent difference in growth compared to the wild type, nor did it show any difference in sensitivity to UV irradiation under our laboratory growth conditions. Overall, these findings indicate that archaeal LOG homologue is active as a phosphoribohydrolase.

IMPORTANCE Lonely Guy (LOG) is an essential enzyme for the final biosynthesis of cytokinins, which regulate almost every aspect of growth and development in plants. LOG protein was originally discovered 12 years ago in a strain of *Oryza sativa* with a distinct floral phenotype of a single stamen. Recently, the presence of LOG homologues has been reported in *Mycobacterium tuberculosis*, an obligate human pathogen. To date, active LOG proteins have been reported in plants, pathogenic and nonpathogenic fungi, and bacteria, but there have been no experimental reports of LOG protein from archaea. In the current work, we report the identification of a LOG homologue active on AMP from *Sulfolobus islandicus* REY15A, a thermophilic archaeon. The protein likely forms a tetramer in solution and represents a novel evolutionary lineage. The results presented here expand our knowledge regarding proteins with phosphoribohydrolase activities and open an avenue for studying signal transduction networks of archaea and potential applications of LOG enzymes in agriculture and industry.

KEYWORDS *Archaea*, *Sulfolobus islandicus*, LOG, phosphoribohydrolase, AMP, cytokinin

Sulfolobus islandicus REY15A is a thermophilic archaeon belonging to the phylum *Crenarchaeota* (1). The members of the *Archaea* domain are ubiquitous and widespread in almost every habitat (2–4). Metagenomic studies have revealed remarkable

Citation Mayaka JB, Huang Q, Xiao Y, Zhong Q, Ni J, Shen Y. 2019. The Lonely Guy (LOG) homologue SiRe_0427 from the thermophilic archaeon *Sulfolobus islandicus* REY15A is a phosphoribohydrolase representing a novel group. Appl Environ Microbiol 85:e01739-19. https://doi.org/10.1128/AEM.01739-19.

Editor Haruyuki Atomi, Kyoto University

Address correspondence to Yulong Shen, yulgshen@sdu.edu.cn.

J.B.M. and Q.H. contributed equally to this article.

Received 29 July 2019
Accepted 10 August 2019
Accepted manuscript posted online 16 August 2019
Published 1 October 2019

diversity and complexity in the physiology of archaea distributed throughout the world (4–6). Although there is no particular report implicating members from archaea as human pathogens, their contribution in areas of biotechnology is important. For example, thermostable enzymes from archaea, such as *Pfu* DNA polymerase from *Pyrococcus furiosus*, are used for DNA amplification by PCR (7). Hence, exploring archaeal enzymes will be of interest for application in other areas, such as in the agricultural sector, industry, and medical fields.

Lonely Guy (LOG) is an enzyme that converts N^6-modified AMP derivatives into N^6-modified adenine free base (cytokinins) and ribose 5-phosphate in a cytokinin-specific phosphoribohydrolase reaction (8). In plants, cytokinins are depicted as cell division promoting molecules (9), and it has been established that LOGs play vital roles in plant growth and development (10, 11), regulating important processes such as apical dominance, leaf senescence, seed dormancy, gametophyte, root proliferation, embryonic development, nutrient signaling, and response to abiotic and biotic factors (12–15). The natural cytokinins (CKs) are composed of core adenine compounds with isoprenoid side chain substituents at the N^6 terminus. In addition to cytokinin, sugar conjugates such as nucleosides, nucleotides, and glucosides are produced. However, biologically active cytokinins are the free base forms in plants, while the less active or inactive conjugates act as storage or translocation sources (12). Cytokinins are chemically referred to as purine bases, which include isoprentyladenine, trans-zeatin, and 6-benzylaminopurine, of which the N^6 atoms are modified with isoprenoid or aromatic rings (16).

Extensive studies of the functions and biosynthesis of cytokinins have been conducted in plants and to a lesser extent in fungi and bacteria. This was partly attributed to incorrect annotations in the database, in which the LOGs were placed as possible lysine decarboxylases (17, 18). Nevertheless, LOG proteins in these organisms have been shown to be key enzymes in the final steps during cytokinin biosynthesis, thus depicting LOGs as essential enzymes in this pathway. For instance, in *Rhodococcus fascians* FAS6, a LOG-like gene has been implicated as a virulence factor causing leafy gall symptom in plants, whereas the IPT-LOG mutant strain failed to cause this symptom (19). Moreover, the ergot fungus *Claviceps purpurea*, a biotrophic pathogen that infects rye ears, was found to produce a significant amount of *de novo* cytokinins during infection (20), but deletion of the *ipt-log* gene of *C. purpurea* did not affect its virulence (20). Furthermore, Samanovic et al. reported that the LOG protein plays a potential role in NO resistance and pathogenesis in the obligate human pathogen *Mycobacterium tuberculosis* (21).

However, no study has been conducted to evaluate archaeal LOG homologues. SiRe_0427 in the hyperthermophilic archaeon *S. islandicus* REY15A was originally annotated as DNA processing protein A (DprA) family in the NCBI database. To investigate possible roles of SiRe_0427, we conducted a bioinformatics survey of its homologues and detected a high level of conservation of the GGGxGTxxE motif. This motivated us to perform a biochemical study of the protein and genetic analysis of *sire_0427* from *S. islandicus*. In this study, we revealed that the SiRe_0427 protein functions as a LOG enzyme, exhibiting hydrolytic activity against AMP, similar to other LOGs from eukaryotes and bacteria. As expected, SiRe_0427 displayed the cardinal features of hydrolytic cleavage of AMP into adenine and ribose 5′-phosphate, a process referred to as dephosphoribosylation. Our preliminary genetic analysis of the *sire_0427* gene showed that the deletion strain did not show any apparent difference in growth and sensitivity to UV irradiation compared to the wild type. Therefore, we provide experimental evidence of the presence of a LOG-homologue protein in archaea, which was designated SisLOG. We finally propose a reclassification of the LOG protein domain.

RESULTS

Presence of conserved LOG motif within SiRe_0427 sequences. SiRe_0427 was originally annotated as DNA processing protein (DprA family) in the NCBI database, which is a protein family that is involved in DNA transformation, recombination, and

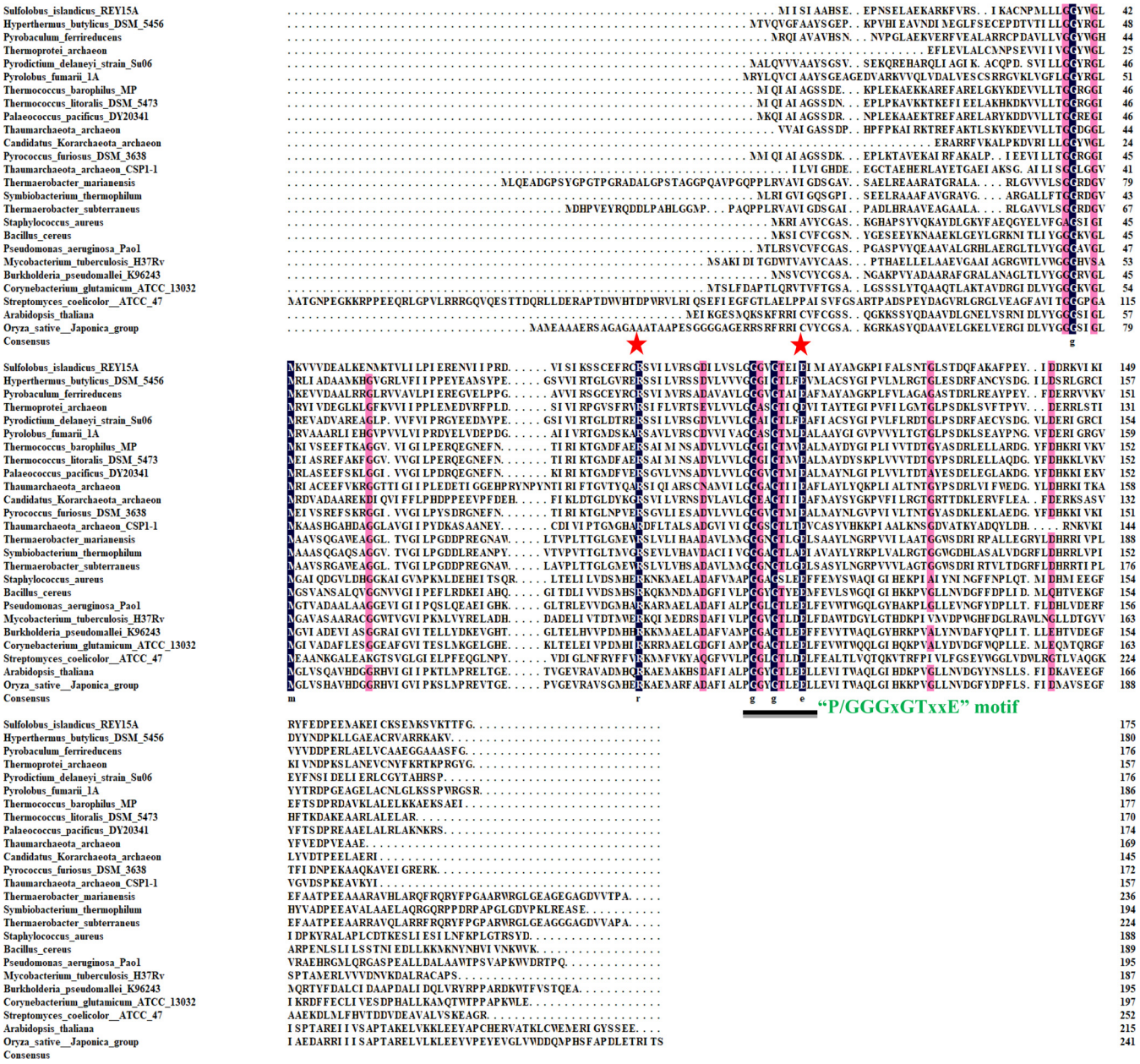

FIG 1 Amino acid sequence alignment of LOG homologues. Twenty-five sequences of representatives of LOG homologues from the three domains of life were analyzed using the DNAMAN server. The names of the species and uncultured groups (*Thermoprotei* archaeon, *Thaumarchaeota* archaeon, and "*Candidatus* Korarchaeota" archaeon) are shown on the left, and the consensus residues are shown at the bottom. The conserved "P/GGGxGTxxE" motif in eukaryotes, bacteria, and archaea is indicated by a black line and green color. The residues for enzyme catalysis are indicated with red stars on top of the residues.

repair. To investigate the possible function of SiRe_0427, we retrieved the SiRe_0427 sequence and other LOG homologues from the NCBI protein database using the BLAST server and then aligned the sequences with the DNAMAN server. A total of 76 representative sequences were obtained, 25 of which were subjected to alignment analysis. We found that the conserved P/GGGxGTxxE motif (where "x" is any amino acid) is present in homologues of all three domains of life (Fig. 1). However, this motif appears to be annotated for two different classes of proteins: Smf/DprA and LOG (22). The PGGxGTxxE motif is conserved in eukaryotes and most bacteria, whereas the GGGxGTxxE motif is present in archaea and some bacteria. It should also be noted that the absence of LOG genes within some phyla or species such as *Escherichia coli* and some obligate intracellular pathogens has been reported (21). However, the DprA

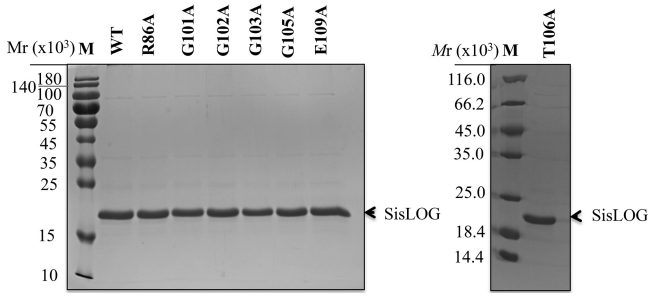

FIG 2 SDS-PAGE analysis of recombinant wild-type SiRe_0427 and mutant proteins. Wild-type SiRe_0427 and seven mutants (12 μg) were loaded onto a 15% gel. The gels were stained with Coomassie brilliant blue after electrophoresis. M, protein molecular standard; M_r, molecular weight.

family proteins share two motifs that are not PGGxGTxxE or GGGxGTxxE motifs. For instance, in *Helicobacter pylori* DprA, the DNA binding motifs are G-S/T/A-R located in (β3-α3) and F/L/Y-x-x-R-N/D located in helix six (α6). *E. coli* O157:H7 strain has two *dprA* paralogs, which possesses an additional A-M-x-R-N/D motif (where "x" is any amino acid) (17, 23). Accordingly, *E. coli* possesses DprA proteins, but not LOG family proteins. Nevertheless, the global distribution of LOG-like homologue genes across the three domains of life reflects the evolutionary importance of LOG domain proteins.

SiRe_0427 has hydrolytic activity on AMP. To determine which class SiRe_0427 protein belongs to, DprA or LOG, we purified wild-type SiRe_0427 protein and conducted biochemical analysis. A total of 7 mg of recombinant enzyme was purified from 2 liters of culture using the *E. coli* BL21(DE3) CodonPlus-RIL strain (Fig. 2). Previous studies have shown that bacterial DprA proteins are involved in transformation through binding of exogenous DNA sequences and protection from nuclease degradation. The newly acquired DNA sequences are incorporated into the recipient genome via DNA recombination together with RecA. For instance, *Helicobacter pylori* DprA is capable of binding to double-stranded DNA (dsDNA) (24), *Rhodobacter capsulatus* DprA can bind to both single-stranded DNA (ssDNA) and double-stranded DNA (dsDNA) (25), and *Streptococcus pneumoniae* DprA is capable of binding to ssDNA alone, with no affinity to dsDNA (26). Our experiments failed to detect DNA (ssDNA and dsDNA) binding activity (data not shown) or an interaction between the SiRe_0427 protein and RadA (Fig. S1), indicating that SiRe_0427 does not function as DprA, which is involved in DNA transformation and recombination, together with RecA in bacteria (23, 26, 27). We next examined whether SiRe_0427 is a functional LOG homologue in *S. islandicus*. Studies have shown that bacterial LOG enzymes are active in hydrolyzing AMP compound *in vitro* (28–30). To test for the phosphoribohydrolase activity of SiRe_0427, we included other substrates in addition to AMP, such as 3′-5′-cyclic AMP (cAMP), ATP, ADP, GMP, UMP, and CMP. The results showed that SiRe_0427 and CgLOG (Cg2612, LOG from *Corynebacterium glutamicum* as a reference enzyme) were unable to hydrolyze cAMP, ATP, ADP, UMP, GMP, and CMP (Fig. S2); however, both CgLOG and SiRe_0427 proteins exhibited activities on AMP (Fig. S3 and Fig. 3). As the reaction time increased, the activity toward AMP of both CgLOG and SiRe_0427 increased (Fig. 3). Notably, at the longest time of 4 or 5 h, nearly all AMP could be hydrolyzed by CgLOG (Fig. S4A and B), whereas only about 35% of the substrate was hydrolyzed by SiRe_0427 (Fig. 3), implying that SiRe_0427 may have a synthesis activity of AMP-like compounds.

To confirm the hydrolytic activity of the wild-type SiRe_0427 protein on AMP substrate, we analyzed the activity with increasing concentrations of the purified wild-type protein. Our results showed that the amount of product formed in the presence of 0.2 μM protein (as monomer) was less than the amount of products formed in the presence of higher enzyme concentrations, with a maximum of 51.2 μM (Fig. 4A and B), and correspondingly, the amount of the substrate decreased as the concentrations of the enzyme increased (Fig. 4A and B). These findings confirm that SiRe_0427 protein is responsible for hydrolyzing the AMP substrate and that the hydrolysis of AMP

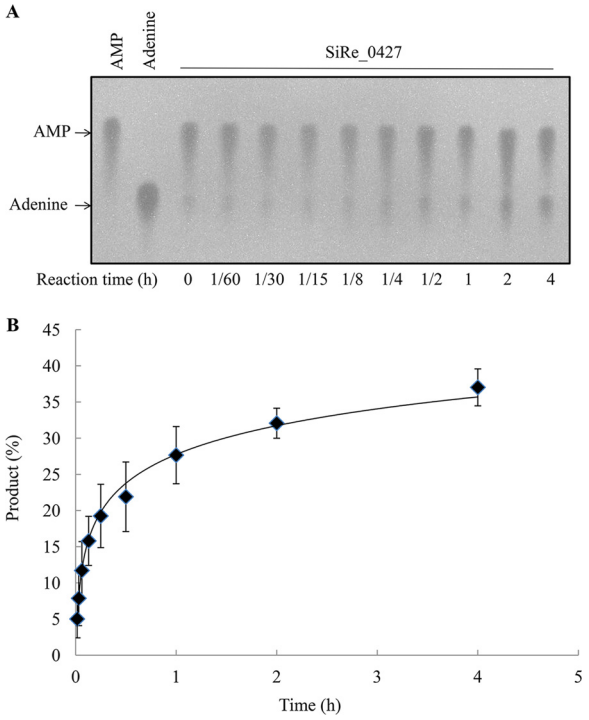

FIG 3 SiRe_0427 exhibits phosphoribohydrolase activity on AMP. (A) Representative profile of the time course of the activity of SisLOG measured by incubating 12.8 μM SisLOG in 20-μl reaction mixtures (pH 7.4) at 65°C. (B) Quantification of the results in panel A. Briefly, 2-μl aliquots of the samples were dotted on TLC sheets, dried, and visualized under a UV lamp at 254 nm. The AMP and adenine standards are in the left two lanes. The reaction time (hours) is indicated at the bottom of the figure. All experiments were repeated at least three times.

substrate occurred in an enzyme-dependent manner. We also checked the enzyme activity of SiRe_0427 using increasing amounts of the AMP substrate (5, 10, 20, 30, 40, and 50 mM), with a constant concentration of the wild-type SiRe_0427 protein (12 μM). Our results showed that, at low concentrations (5, 10, 20, and 30 mM), the amount of the products formed in an incremental manner. However, with further increases in the substrate, the reaction product appeared to remain unchanged (Fig. 4C and D). In addition, we assessed the phosphoribohydrolase activity of the wild-type SiRe_0427 enzyme at temperatures ranging from 25 to 85°C (Fig. S4A and B). As expected, SiRe_0427 protein exhibited phosphoribohydrolase activity at a wide range of temperatures, with pronounced activity against AMP substrate, especially at 65 to 85°C (Fig. S4A and B).

Finally, to check whether the conserved residues are involved in enzyme catalysis or AMP binding sites, we obtained mutant proteins by site-directed mutagenesis (Fig. 2) and performed similar experiments as described above. As expected, the alanine mutants R86A, G101A, G102A, G105A, T106A, and E109A lost their enzyme activity against the AMP substrate (Fig. 5A and B), indicating that these residues are involved in either enzyme catalysis or substrate binding. These results are generally in agreement with those reported for bacterial LOGs (28–30). Interestingly G101A lost its activity, while mutant G103A exhibited a similar enzyme activity against AMP substrate as the wild type (Fig. 5). This was likely because the archaeal LOG motif GGGxGTxxE starts with G101 as its first residue, while LOGs of eukaryotes and most bacteria have proline (P) as their initial residue, which is not involved in binding of AMP substrate. Apparently, the AMP molecule binding sites could have shifted from G103 to the G101. As such, G103 could not access the AMP molecule and was therefore not involved in binding of the AMP substrate (Fig. 5; see also Fig. S5A). This situation was not observed in species possessing the PGGxGTxxE motif. Evaluation of the mutant activity revealed

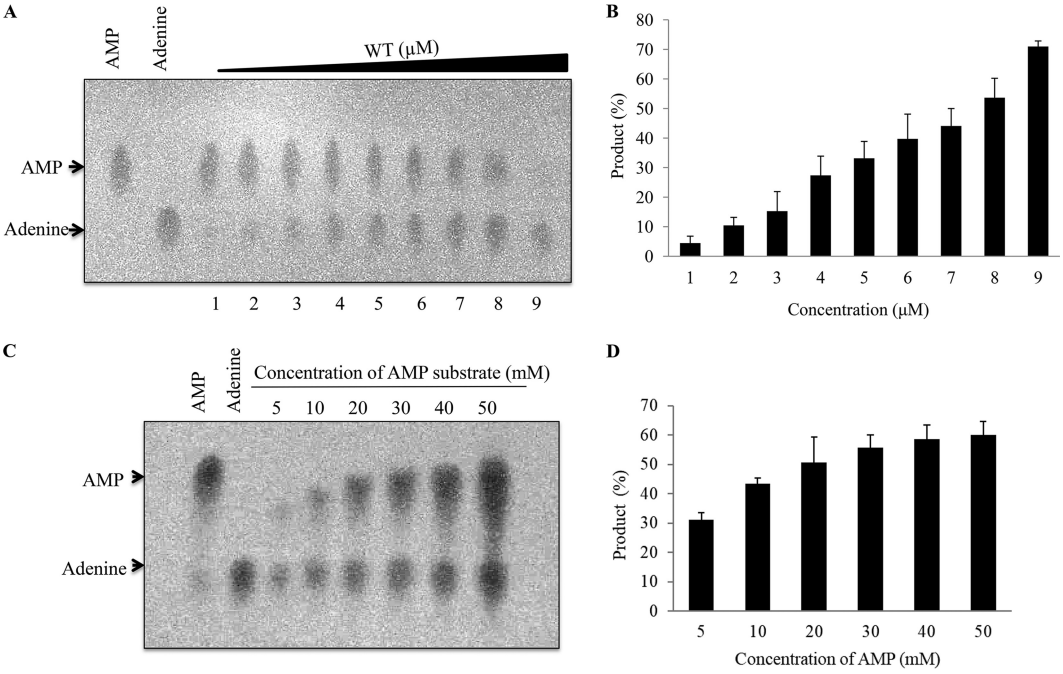

FIG 4 Analysis of the phosphoribohydrolase activity of SiRe_0427 with increasing concentrations of protein and substrate. (A) Phosphoribohydrolase activity of SiRe_0427 as a function of concentrations. The experiment was performed using increasing concentrations of wild-type SiRe_0427 protein (columns 1 to 9: 0.2, 0.4, 0.8, 1.6, 3.2, 6.4, 12.8, 25.6, and 51.2 μM, respectively) and 20 mM AMP substrate. The 20-μl reaction mixtures (pH 7.4) were incubated at 65°C for 3 h. (B) Quantification of the results in panel A using ImagQuant. (C) Phosphoribohydrolase activity of SiRe_0427 protein with increased concentrations of AMP. The reaction was performed at 65°C using 12 μM SiRe_0427 protein and increasing concentrations of AMP (5, 10, 20, 30, 40, and 50 mM) in 20-μl reaction mixtures (see Materials and Methods). One to two microliters of samples was dotted onto each TLC sheet. After separation, the plate was dried and visualized by UV illumination at 254 nm. The AMP and adenine standards are on the left side of the figure. (D) Quantification of the results in panel C. The reaction time (hours) is indicated at the bottom of the figure. All experiments were repeated at least three times.

slight differences in the function of conserved residues between SiRe_0427 and other reported LOGs and further confirmed that SiRe_0427 is responsible for the phosphoribohydrolase activity. Therefore, based on our results we conclude that SiRe_0427 is a LOG homologue in *S. islandicus*; hence, it is here referred to as SisLOG.

Determination of the oligomeric status of SisLOG. Lonely Guy (LOG) proteins have been reported as either dimers or hexamers (29). To determine whether archaeal

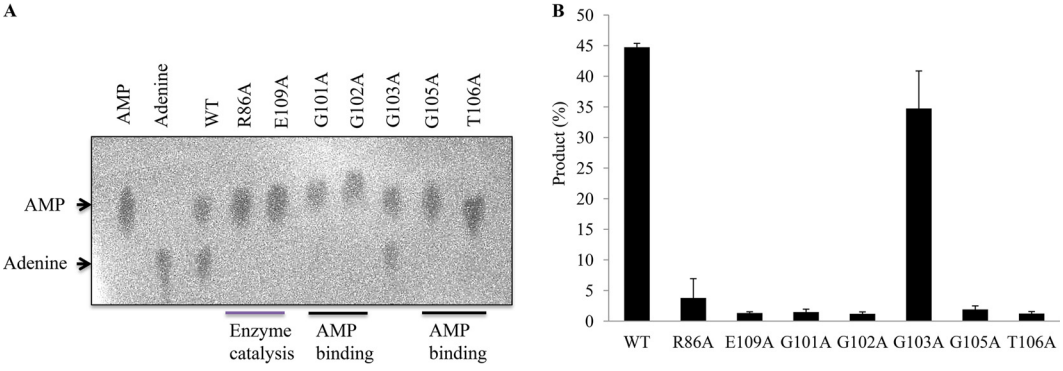

FIG 5 Analysis of the phosphoribohydrolase activity of SiRe_0427 mutants on AMP. (A) The catalytic and substrate binding mutants lost their phosphoribohydrolase activity on AMP. The reaction was performed at 65°C and pH 7.4 for 4 h (see Materials and Methods). One to two microliters from the mixture was then dotted onto a TLC sheet. After separation, the plate was dried and visualized by UV illumination at 254 nm. (B) Quantification of the results in panel A. The AMP and adenine standards are on the left side of the figure. The reaction times (hours) are indicated at the bottom of the figure. All experiments were repeated at least three times.

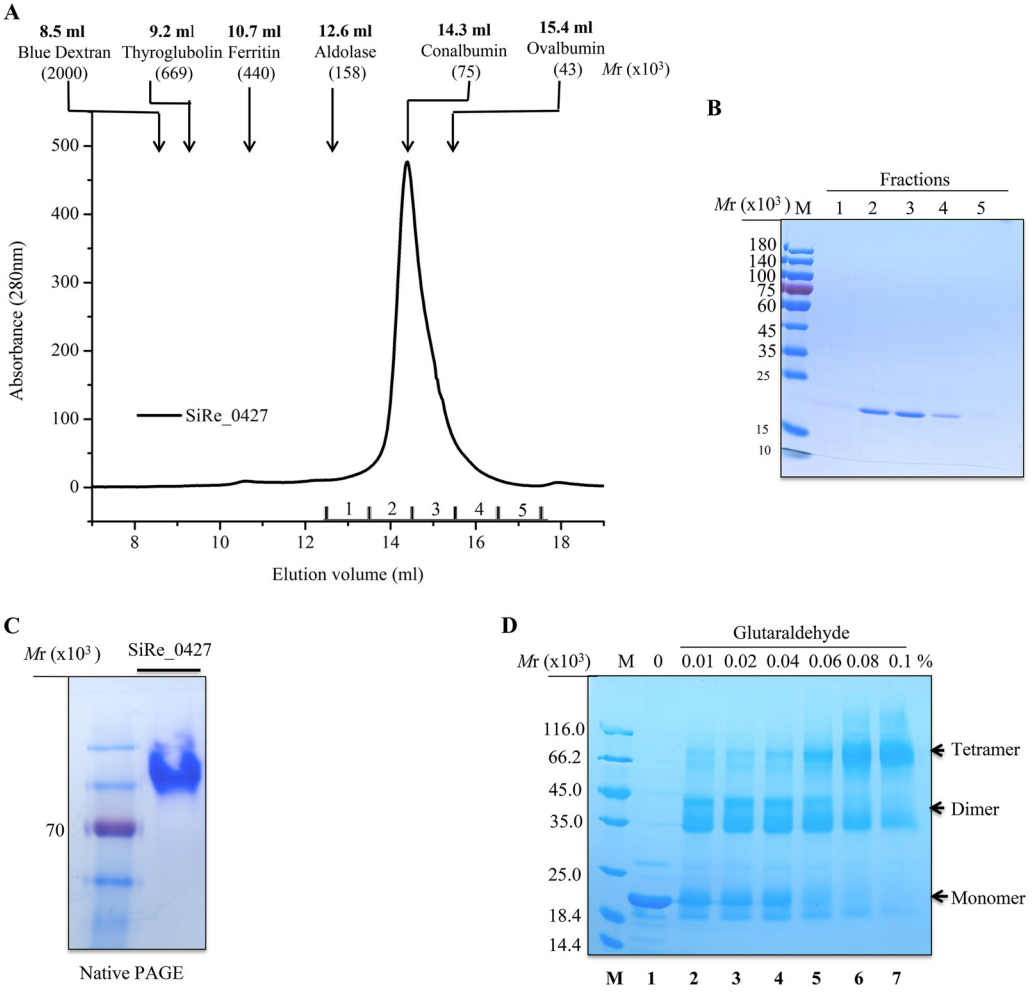

FIG 6 Confirmation of the oligomeric status of the wild-type SiRe_0427 protein using chemical cross-linking and native PAGE analysis. (A) Size exclusion profile of wild-type SiRe_0427. The protein (3.8 mg/ml) in a buffer of 50 mM Tris-HCl (pH 7.4), 200 mM NaCl, 5% glycerol, and 1 mM DTT was loaded onto a Superdex 200 column. The protein standards are indicated with arrows. (B) SDS-PAGE of peak fractions in panel A. The gel was stained with Coomassie brilliant blue. M, molecular size markers. (C) Native PAGE analysis of the purified recombinant wild-type SiRe_0427 protein (18 μM) with 8% gel. An SDS-PAGE marker (Thermo Fisher Scientific, catalog no. 26616) was used to indicate the relative position of the protein in the gel. The marker included one protein corresponding to an M_r of $\sim 70 \times 10^3$ (red). (D) SDS-PAGE analysis of cross-linking samples using increasing concentrations of glutaraldehyde with a final concentration of 0.1%. The samples were analyzed on a 15% SDS-PAGE gel. M, molecular size standard. Lanes: 1, no cross-linking agent; 2 to 7, increasing concentrations of cross-linker. The oligomer species are indicated on the right of the figure.

SisLOG falls within the established clusters of dimeric or hexameric LOG proteins, we used size exclusion chromatography to assess the oligomeric status of the purified wild-type SisLOG (M_r 19.5×10^3 as a monomer). SisLOG eluted at 14.3 ml, corresponding to a protein with molecular weight of 75×10^3, which is close to a tetramer of SisLOG (78×10^3; Fig. 6A and B). Similarly, all mutant proteins eluted at the same position as the wild type in a single peak (data not shown). These findings suggested that SiRe_0427 protein forms a homotetramer in solution. Interestingly, this result is in agreement with a modeling structure of SiRe_0427 (Fig. S6). We also checked the oligomer status of SiRe_0427 by native PAGE and found that the protein appeared in a single band (Fig. 6C), indicating that the homotetramer is a stable state of the protein.

To gain more insight into the self-association level of SiRe_0427 protein, we conducted a cross-linking experiment using purified recombinant wild-type SisLOG protein (18 μM) and glutaraldehyde. After the cross-linking treatment, the wild-type SiRe_0427 protein showed migration bands of approximately 19.5×10^3, 39×10^3, and 78×10^3, corresponding to a monomer, dimer, and tetramer, respectively (Fig. 6D).

TABLE 1 Oligonucleotides used in this study[a]

Primer	Sequence (5′–3′)[b]	Site[c]
0427-F	CATCCACCATATGATCATTTCCATAGCAGC	NdeI
pSeSD-0427-R	GACGGTCGACTTAGCCGAAAGTAGTCTTC	SalI
pK-0427-F (TG-arm)	CTCAGTCGACATGCTGCTTTTAGGAGGATA	SalI
pK-0427-R (TG-arm)	AACCACGCGTTTAGCCGAAAGTAGTCTTCA	MluI
pK-0427-F (L-arm)	CACGCCATGGTCGAGAACAACAGTAATGT	NcoI
pK-0427-R (L-arm)	GGAGCTCGAGGAATAGTAAATCCTTTCATC	XhoI
pK-0427-F (R-arm)	GCTTCTCGAGCTACTTTCGGCTAAGCTT	XhoI
pK-0427-R (R-arm)	GAATGCATGCGCAATGCAGAGCCTGCAGTA	SphI
Flank-0427-F	AAATTCGGACTTCTTACCACCATAGG	
Flank-0427-R	GTTGAAAGGGAATTTACGAGTGATCC	
CgLOG-F	GCGCCATATGACTTCGCTTTTCGACGCCCC	NdeI
CgLOG-R	GCGCGTCGACCCATTTTGGTGCTGGTGGAGTCC	SalI
0427-R86A-F	TGTGAGTTTAGATGCGCATCCGTAATCCTTGT	
0427-R86A-R	ACAAGGATTACGGATGCGCATCTAAACTCACA	
0427-G101A-F	ATACTAGTTTCATTGGCAGGAGGTGTTGGAACGG	
0427-G101A-R	CCGTTCCAACACCTCCTGCCAATGAAACTAGTAT	
0427-G102A-F	CTAGTTTCATTGGGAGCAGGTGTTGGAACGGA	
0427-G102A-R	TCCGTTCCAACACCTGCTCCCAATGAAACTAG	
0427-G103A-F	GTTTCATTGGGAGGAGCTGTTGGAACGGAAA	
0427-G103A-R	TTTCCGTTCCAACAGCTCCTCCCAATGAAAC	
0427-G105A-F	ATTGGGAGGAGGTGTTGCAACGGAAATAGAAAT	
0427-G105A-R	ATTTCTATTTCCGTTGCAACACCTCCTCCCAAT	
0427-T106A-F	TGGGAGGAGGTGTTGGAGCGGAAATAGAAATAATG	
0427-T106A-R	CATTATTTCTATTTCCGCTCCAACACCTCCTCCCA	
0427-E109A-F	GGAACGGAAATAGCAATAATGATTGCTTACGC	
0427-E109A-R	GCGTAAGCAATCATTATTGCTATTTCCGTTCC	

[a]Abbreviations: TG-arm, target gene arm; L-arm, left sequence to target gene; R-arm, right sequence to target gene; F, forward; R, reverse.
[b]Underlined sequences represent restriction enzyme cutting sites.
[c]Restriction enzyme.

With increasing concentrations of glutaraldehyde, the SiRe_0427 protein apparently formed higher-molecular-weight oligomers (Fig. 6D, lanes 6 and 7), but with simultaneous reduction of the monomeric form. Therefore, this result concurred with that of the gel filtration analysis. Taken together, the size exclusion chromatography and chemical cross-linking results were in agreement with the tetramer model structure of SiRe_0427 (Fig. S6). Although the crystal structure of SiRe_0427 has not been determined, we suggest that SiRe_0427 protein exists as a homotetramer in solution.

Genetic analysis of SiRe_0427. To understand the *in vivo* function of SiRe_0427, we conducted genetic analysis of the gene utilizing the marker insertion and target gene deletion (MID) method to knock out the *S. islandicus* REY15A *sire_0427* gene (31). The integration of pMID-*sire_0427* plasmid into the *S. islandicus* genome was confirmed by PCR using SiRe_0427-Flanking forward/reverse primers (Table 1; see also Fig. S7 in the supplemental material). After a series of screening and counterselection procedures, the *sire_0427* deletion mutant strain was obtained. The genotype of the *sire_0427* knockout strain was verified by PCR using the Δ*sire_0427* genomic DNA and three pairs of primers (SiRe_0427-Flank-forward/SiRe_0427-Flank-reverse, SiRe_0427-Gene-forward/reverse, and SiRe_0427-Gene-forward/Flank-reverse; Table 1 and Fig. 7). Thus, the *sire_0427* gene can be deleted from *S. islandicus* REY15A. However, we were unable to see any apparent difference in growth between the Δ*sire_0427* strain and the wild type in liquid medium or on solid plates (Fig. 8).

To determine whether SiRe_0427 is involved in DNA damage repair, we tested the UV irradiation sensitivity of the knockout strain by spot assay on MCSVU plates (mineral salt medium supplemented with 0.2% [wt/vol] Casamino Acids, 0.2% [wt/vol] sucrose, a mixed-vitamin solution, and 0.01% [wt/vol] uracil) (31). The inoculated plates were exposed to different dosages of UV irradiation (10, 20, and 30 J/m^2). Observation of the growth of the wild-type and Δ*sire_0427* strains after incubation at 75°C for 7 days revealed no significant difference among UV dosages (Fig. 8B), indicating that

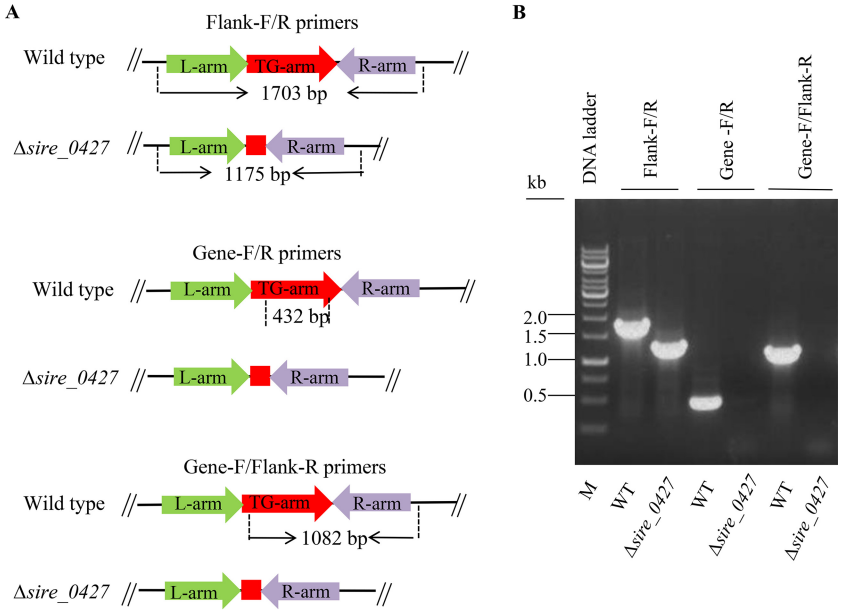

FIG 7 Gene knockout and analysis of Δ*sire_0427* strain by PCR. (A) Schematics showing the theoretical gene length of *sire_0427* and flanking sequences. (B) Verification of gene deletion by PCR. The PCR mixture contained 200 ng of genomic DNA of *sire_0427* in 25-μl samples and specific primers. The samples were analyzed by electrophoresis in a 1% agarose gel.

SiRe_0427 is not directly involved in DNA damage repair and confirming that it was not a DprA homologue.

Phylogenetic tree analysis. Our *in vitro* biochemical results demonstrated that SisLOG (or archaeal LOGs) may represent a new group of the existing classification of LOG protein domains, since no reported bacterial or eukaryotic LOGs function as tetramers. To further explore the relationship between archaeal LOGs and those from eukaryotes and bacteria, the evolutionary history was inferred by construction of a phylogenetic tree of 76 representative SiRe_0427 homologues using the unrooted maximum-likelihood method and the JTT matrix-based model. We found that LOGs fell into several distinct groups (Fig. 9). Interestingly, those of archaea and some thermophilic bacterial LOG homologues contained the invariant glycine sharing GGGxGTxxE motif and were clustered together (Fig. 9). The remaining proteins from eukaryotes and mesophilic bacteria all contained the PGGxGTxxE motif, with plant LOGs clustering together into a clear branch, mesophilic bacterial homologues forming a group, and fungal homologues clustering into a nearly distinct third group (Fig. 9).

DISCUSSION

DNA processing protein A (DprA) and LOG were mistakenly annotated as sharing similar motifs, even though they have similar biochemical features such as binding to DNA/RNA oligonucleotides as observed in the DprA/Smf family or NMPs in the LOG family (22). Burroughs et al. revealed a genetic network by comparative genomic analysis (22) in which DprA and LOG-related proteins comprised a superfamily known as SLOG (for Smf/DprA and LOG proteins). This superfamily includes five clades and 15 families, among which only three families have been characterized, DprA/Smf, LOGs, and the molybdenum cofactor-binding (MoCoBD) family (22). Our study revealed that SiRe_0427 in the TPALS (TIR/PNP-associating LOG-DprA/Smf) family is a phosphoribohydrolase similar to LOG homologue proteins that have been reported in eukaryotes and bacteria (8, 10, 11, 21, 26, 28, 30). These findings indicate that phosphoribohydrolases are widely distributed in all the three domains of life. It is not clear what the actual substrate of the SisLOG enzyme is. One possibility is that the substrate of SisLOG is a precursor of cytokinin-like compound or oligonucleotide (ssDNA, RNA, linear, or circu-

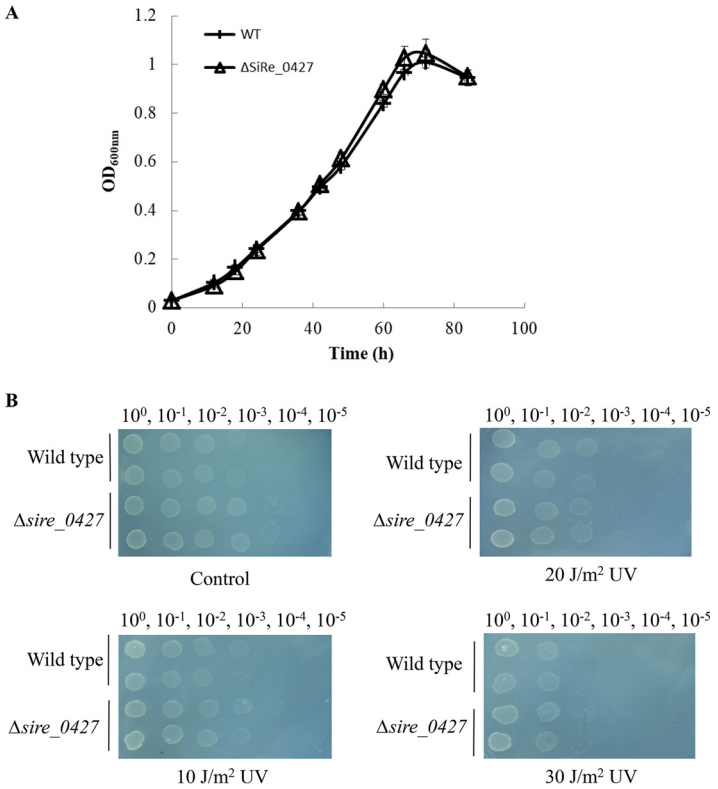

FIG 8 Growth curves and DNA damage sensitivity analysis of *S. islandicus* Δ*sire_0427* strain. (A) Growth curves of the wild-type and Δ*sire-0427* strain grown on MCSVU liquid medium. (B) UV sensitivity analysis of the wild-type and Δ*sire_0427* strains by spot assay. The plates were exposed to UV irradiation (10, 20, and 30 J/m^2) on MCSVU plates after being spotted with cultures at an OD_{600} of 0.2 and incubated at 75°C for 7 days.

lar). The enzyme could catalyze the generation of putative cytokinin in archaea and some thermophilic bacteria. Further study is needed to isolate and identify cytokinin-like compounds from the cells. The other possible kind of substrates of SisLOG is small signal molecule, like cyclic-di-AMP (c-di-AMP), c-di-GMP, or c-GAMM. Again, isolation of the compounds and testing whether SisLOG is active toward them will be needed. We assume that SisLOG is an important enzyme in generation, sensation, and regulation of signal molecules. Supporting this is the finding that there are nucleotide molecules in archaea such as cyclic-di- and linear oligonucleotide signals, which have functions that have only just begun to be elucidated (32, 33). We also do not know in what cellular process SisLOG is involved. We found that *sire_0427* can be deleted (Fig. 7); however, there was no apparent difference in the growth and sensitivity to UV irradiation between wild-type and Δ*sire_0427* strains under the standard growth conditions as for *S. islandicus* REY15A (Fig. 8). We checked for neighbor genes and found that the surrounding genes were hypothetical proteins with unknown functions. In the upstream area, there is a gene encoding ABC transporter, which could serve as a transporter of signal molecules. It is likely that some of these neighbor gene products function in sensing and regulation of signals. However, further study is needed to address these questions.

Our structural comparison revealed topological fold arrangement of SiRe_0427 similar to that reported for *Corynebacterium glutamicum* LOG (CgLOG, PDB 5WQ3) (28), especially at the motif region (Fig. S5B). However, unlike eukaryotic LOGs, archaeal and some bacterial LOG homologues such as those from *Thermaerobacter marianensis*, *Thermaerobacter subterraneus*, and *Symbiobacterium thermophilum* shared the GGGxGTxxF motif, which contains consecutive triple glycine (G) residues and has a first residue consisting of glycine instead of proline (P), as in all eukaryotic and bacterial LOGs that have been reported to date.

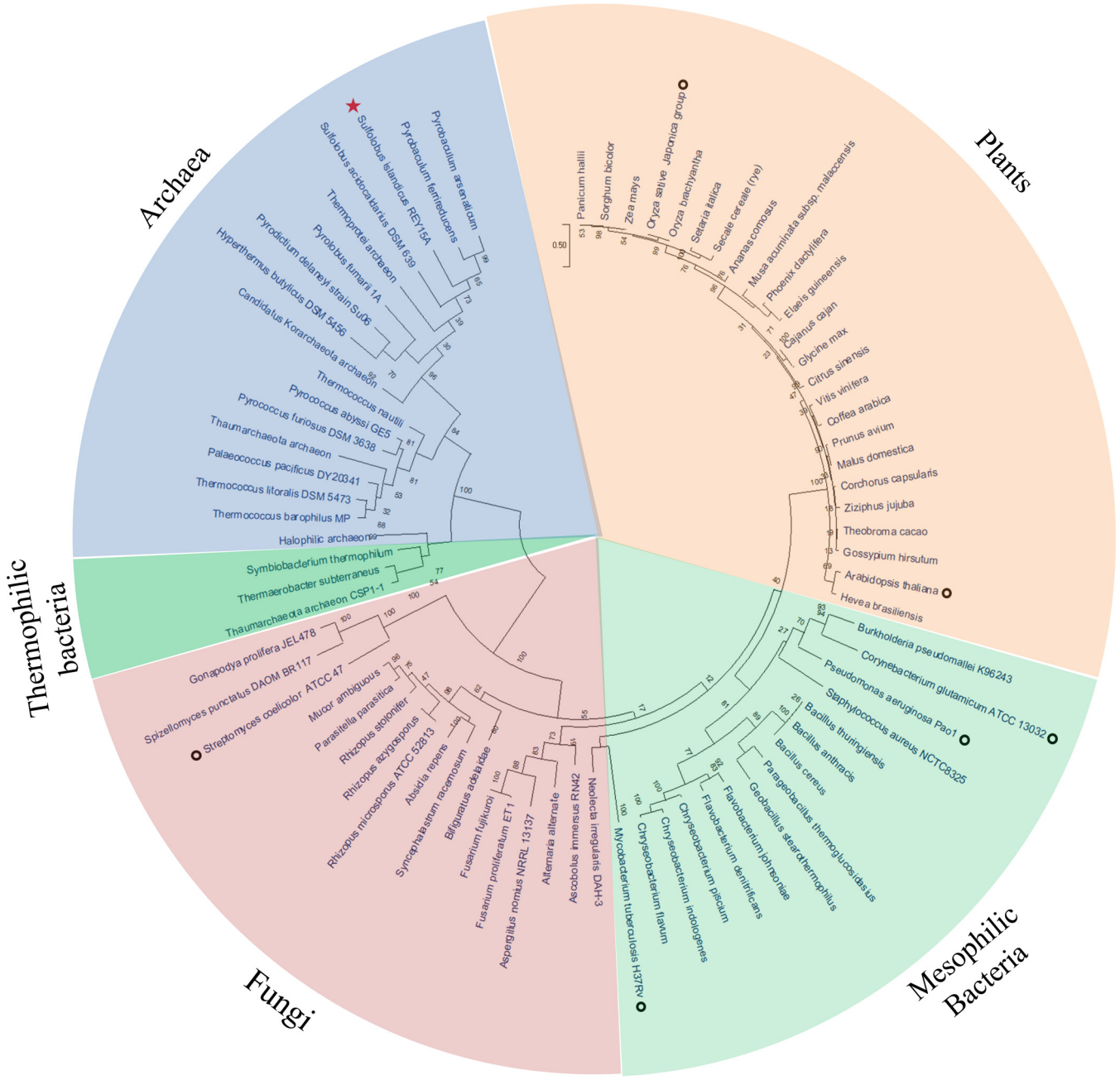

FIG 9 Phylogenetic tree of LOG proteins from the three domains of life. The unrooted maximum-likelihood method (40) was used to generate a phylogenetic tree with the MEGA X server (39). The circular model tree comprised 76 representative LOG homologue sequences from eukaryotes, bacteria, and archaea (including four uncultured groups, *Thermoprotei* archaeon, *Thaumarchaeota* archaeon, "*Candidatus* Korarchaeota" archaeon, and halophilic archaeon), and all amino acid sequences from Fig. 1 are included. Bootstrap values are indicated at each junction (node) as percentages. The red star indicates *S. islandicus* REY15A strain used in the present study, and open black circles indicate strains from eukaryotes (8, 10, 11) and bacteria (21, 26, 28, 30) for which phosphoribohydrolase activities have been reported.

The LOG proteins have been classified into two clusters: dimeric and hexameric (29). Further, the cluster of dimeric LOGs was assigned as type I LOGs and the cluster of hexameric LOGs as type II LOGs, each of which contained subtypes (Ia, Ib, IIa, and IIb, respectively). This classification is based on the phylogenetic analysis, oligomerization status of LOG proteins, and residues involved in catalysis (29). Interestingly, no members from archaea were mentioned because archaeal LOG homologues were still in limbo. However, our study identified a LOG homologue from *S. islandicus* REY15A as a tetramer (Fig. 6; see also Fig. S6 in the supplemental material), which was exclusive of the two clusters proposed on the basis of protein oligomerization (29).

To get insight into the oligomer formation mechanism, the subunit interaction interfaces were compared based on the crystal structures of CgLOG I (dimer, PDB 5ITS), CgLOG II (hexamer, PDB 5WQ3), and the model of SisLOG (tetramer). Superposition of three structures revealed that the monomeric structures were remarkably similar, although the similarity among the three LOG protein sequences is quite low (Fig. S8). Different polar contact residues between the chains of CgLOG I and II dimers were identified (e.g., Y27, K100, and E125 for CgLOG I [Fig. S9]; the corresponding residues are Y85, K156, and E181 in CgLOG II). The sites involved in the subunit interaction of SisLOG were totally different, although it was located at the same interface (Fig. S10). Each monomer of SisLOG had two distinct groups of residues for the interactions with other adjacent subunits, leading to a distinct tetramer formation for SisLOG (Fig. S10 and S11). Three CgLOG II dimers were further organized into a hexamer mediated through the additional helix of each monomer (Fig. S11).

Therefore, we would suggest that if cluster 1 LOGs consist of dimeric forms, then cluster 2 should contain tetrameric LOGs and hexameric LOGs should shift to cluster 3 instead of cluster 2 as previously proposed (29). On this basis, we would propose cluster 1 (dimers), cluster 2 (tetramers), and cluster 3 (hexamers). However, as we detected the presence of the GGGxGTxxE motif in some bacterial species such as *T. marianensis*, *T. subterraneus*, and *S. thermophilum*, it is not clear whether these bacterial species share similar oligomeric status with *Sulfolobus* (archaea) as tetramers or not. Future studies are needed to acquire experimental evidence to provide a comprehensive classification of LOG protein domains.

In conclusion, we identified an archaeal LOG with an oligomeric status as a tetramer. Further investigations of archaeal LOGs are needed to unravel the cellular function and structure and to identify possible archaeal cytokinin types and biosynthesis pathways.

MATERIALS AND METHODS

Sequence alignment and databases. The SiRe_0427 DNA and protein sequences were retrieved from the National Center for Biotechnological Information (NCBI) site and the Protein Data Bank (34). Sequence analysis was performed by local alignment searches using BLAST/PSI-BLAST (35) and/or Muscle 3.7 and CLUSTAL2 (36, 37). Multiple sequence alignment was conducted by using the PSI-BLAST and/or DNAMAN servers. Secondary structure prediction of SiRe_0427 protein was performed by phyre^2 (38) and SiRe_0427 structure modeling was conducted by the SWISS-MODEL Server. The protein monomeric and tetrameric structural comparisons were performed and visualized in the PyMOL server (http://www.pymol.org). The unrooted maximum-likelihood method and JTT matrix-based modeling were used to construct a phylogenetic tree using the MEGA X server (39, 40).

Reagents, strains, plasmids, and culture conditions. All chemicals and reagents used in this study were of analytical and molecular biology grades. IPTG (isopropyl-β-D-thiogalactopyranoside) and ampicillin were purchased from Clontech (Shiga, Japan), and chloramphenicol was obtained from Sangon Biotech (Shanghai, China). dATPs, ATP, cAMP, ADP, GMP, CMP, and UMP were acquired from Sigma (St. Louis, MO), whereas dithiothreitol (DTT), adenine, and AMP were obtained from BBI Life Sciences (Shanghai, China). Restriction enzymes were from TaKaRa (Shiga, Japan). Glutaraldehyde was from Sinopharm Chemicals (Shanghai, China), TLC PEI cellulose F and TLC silica plates 60F$_{254}$ were purchased from Merck (Darmstadt, Germany), and agarose was obtained from Invitrogen (Waltham, MA).

The wild-type *S. islandicus* REY15A strain and *S. islandicus* E233S (*pyrEF lacS* double mutant) were used as the original and wild-type strains, respectively (31, 41). *E. coli* DH5α strain was grown in Luria-Bertani (LB) medium supplemented with ampicillin (100 μg/ml) if required. *E. coli* BL21(DE3) CodonPlus-RIL was grown on LB medium supplemented with 100 μg/ml ampicillin and 24 μg/ml chloramphenicol for use as a host for overexpression of a hexa-histidine (6×His)-tagged protein at the C terminus using pET22b.

Construction of the plasmids. The *S. islandicus* SiRe_0427 gene was amplified by PCR using *Pfu* DNA polymerase (TransGen) from the genomic DNA of *S. islandicus* REY15A as a template and the primers 5′-CATCCACCATATGATCATTTCCATAGCAGC-3′ (forward) and 5′-ACCAGTCGACGCCGAAAGTAGTCTTCAC AC-3′ (reverse, no stop codon) carrying NdeI and SalI enzyme restriction sites, respectively. The PCR product was gel purified and digested with NdeI and SalI restriction enzymes. The DNA fragment was extracted using a gel extraction kit and then ligated by T4 DNA ligase (TaKaRa) into the NdeI-SalI restriction sites of pET22b vector, generating pET22b-SiRe_0427-C-His (Table 2). The size of the inserted DNA fragment was verified by restriction enzyme digestion and running of the sample on 1% agarose gel. The sequence in the construct was confirmed by sequencing (BGI, Shenzhen, People's Republic of China; Sangon, Shanghai, People's Republic of China).

Plasmids for expression of site-directed mutants were constructed by splicing overlap extension PCR with oligonucleotide primers (Table 1), and the DNA fragments of each mutant were digested with corresponding enzymes and ligated by T4 DNA ligase into the NdeI and SalI sites of pET22b. All plasmid constructs were verified by double enzyme digestion and confirmed by sequencing.

TABLE 2 Strains and plasmids used and constructed in this study

Strain	Characteristics/usage	Source or reference
S. islandicus REY15A	Wild type	Contursi et al. (41)
S. islandicus REY15A (E233S)	Δ*pyrEF-lacS*	Deng et al. (31)
S. islandicus Δ*sire_0427*	Δ*pyrEF-lacS* Δ*sire_0427*	This study
E. coli DH5α	Plasmid amplification	Laboratory strain
E. coli BL-21(DE3) codon plus-RIL	Protein expression	Laboratory strain
E. coli/pET22b-SiRe_0427-C-His	Wild-type SiRe_0427	This study
E. coli/pET22b-SiRe_0427R86A-C-His	R86A (catalytic mutant)	This study
E. coli/pET22b-SiRe_0427G101A-C-His	G101A (substrate binding mutant)	This study
E. coli/pET22b-SiRe_0427G102A-C-His	G102A (substrate binding mutant)	This study
E. coli/pET22b-SiRe_0427G103A-C-His	G103A (activity similar to that of the wild type)	This study
E. coli/pET22b-SiRe_0427G105A-C-His	G105A (substrate binding mutant)	This study
E. coli/pET22b-SiRe_0427T106A-C-His	T106A (substrate binding mutant)	This study
E. coli/pET22b-SiRe_0427E109A-C-His	E109A (catalytic mutant)	This study

Protein purification. To purify wild-type SiRe_0427 and its mutant proteins from the *E. coli* BL-21 (DE3) CodonPlus-RIL strain, cells were grown in 2 liters of LB medium at 37°C with shaking until the optical density at 600 nm (OD_{600}) was ~0.7, after which 1.0 mM IPTG was added; the cells were then grown at 18°C for 16 h with shaking. The cells were subsequently harvested by centrifugation at 6,000 × *g* for 10 min and then resuspended in lysis buffer A (50 mM Tris-HCl [pH 7.4], 200 mM NaCl, 1 mM DTT, and 5% glycerol). Next, the cells were disrupted by sonication, and the cell debris was removed by centrifugation at 12,000 × *g* for 30 min. The supernatant was incubated at 70°C for half an hour, centrifuged, and then filtered through a membrane filter (0.45-μm pore size) and loaded onto a Ni-NTA agarose column (Invitrogen) that was preequilibrated with buffer A. Protein impurities were removed by washing with buffer A containing 40 mM imidazole, and the bound protein was eluted with buffer A containing 300 mM imidazole. The eluted sample was analyzed using a 15% SDS-PAGE gel and then concentrated by ultrafiltration using Amicon Ultra-15 concentrators (Millipore). Additional purification steps were performed by HiTrap QFF ion-exchange chromatography and size exclusion chromatography (Superdex 200 10/300 column; GE Healthcare Bio-Science). Protein fractions were pooled, and the concentration was determined by the Bradford method using bovine serum albumin as the standard. Recombinant CgLOG (~20 mg) was purified from 1 liter of LB culture in *E. coli* with a buffer containing 50 mM Tris-HCl (pH 8.0), 200 mM NaCl, 1 mM DTT, and 5% glycerol. The proteins were either immediately used for *in vitro* assays or frozen with liquid nitrogen and stored at −80°C for subsequent use. All buffer pHs were prepared and adjusted at room temperature.

SDS-PAGE and native-PAGE analyses. To determine the purity and molecular size of recombinant wild-type SiRe_0427 and its mutant proteins, 12 μg of either wild-type or mutant proteins was applied to a 15% PAGE gel containing 0.1% SDS under reducing conditions. To check the oligomerization status of wild-type SiRe_0427 and its mutant proteins, 12 μg of each protein was loaded onto an 8% native-PAGE gel. Gels were stained with Coomassie brilliant blue R-250 after electrophoresis.

***In vitro* pulldown assay.** His-tagged SiRe_0427 of 5.2 and 6.4 μM untagged RadA proteins were mixed in a 600-μl reaction mixture and then incubated at 65°C for 30 min. The mixture was subsequently applied onto 150 μl of Ni-NTA beads that had been preequilibrated with buffer A (50 mM Tris-HCl [pH 7.4], 200 mM NaCl, 5% glycerol), followed by incubation at room temperature for 20 min by gentle swirling. The sample was then centrifuged at 3,000 × *g* for 5 min, and the pellet was washed three times with buffer A containing 40 mM imidazole. The proteins were subsequently eluted with buffer A containing 300 mM imidazole and then assessed by SDS–15% PAGE. Next, samples containing 3 mg/ml of each His-tagged SiRe_0427, RadA, or mixtures of His-tagged SiRe_0427 and untagged-RadA with 2 ng of 34-mer ssDNA or without the oligonucleotides were incubated at 65°C for 30 min. The mixture was loaded onto a Superdex 75, 10/300 gel filtration column (GE Healthcare) that had been preequilibrated with buffer B (50 mM Tris-HCl [pH 7.4], 150 mM NaCl, and 5% glycerol). Finally, the fractions were assessed by SDS–15% PAGE.

Chemical cross-linking assay. Chemical cross-linking of SiRe_0427 and its mutant proteins was conducted as previously reported (42, 43). Briefly, glutaraldehyde was used as a chemical cross-linker to covalently cross-link protein subunits via primary amines of lysine residues. Wild-type SiRe_0427 and mutant proteins were incubated with increasing concentrations of glutaraldehyde (0.01 to 0.1%) on ice at 4°C for 15 min. The reaction was then stopped by addition of SDS-PAGE loading buffer, after which the samples were electrophoresed by SDS–15% PAGE or native– 8% PAGE, and the gels were stained with Coomassie brilliant blue R-250.

Phosphoribohydrolase activity assay. A phosphoribohydrolase activity assay was performed according to Seo et al. (28), with slight modifications. Briefly, reaction mixtures (20 μl) consisting of 20 mM concentrations (each) of the following substrates were prepared: AMP, cAMP, ATP, ADP, GMP, UMP, or CMP in either 36 mM Tris-HCl (pH 7.4) and 12.8 μM purified wild-type SiRe_0427 and its mutant proteins or 36 mM Tris-HCl (pH 8.0) and 8 μM CgLOG protein at room temperature. The reaction mixtures were incubated at 65 or 37°C for different times as specified. The reaction was stopped by heating the sample at 98°C for 5 min, after which 1 to 2 μl of the reaction samples was dotted onto a PEI-cellulose-F plastic thin-layer chromatography (TLC) sheet (Merck Millipore, Germany). Sodium chloride (NaCl, 1 M) was used as the mobile phase, and the sheet was developed in a TLC chamber and air dried. The adenine

compound was then detected by UV illumination at 254 nm, and the image was analyzed by UVP Bio-Imaging Systems (CA). *Corynebacterium glutamicum* LOG (CgLOG) was used as the control. All experiments were conducted in triplicate.

SiRe_0427 activity as a function of enzyme and substrate concentrations. Experiments were conducted with increasing concentrations of the wild-type SiRe_0427 protein (0.2, 0.4, 0.8, 1.6, 3.2, 6.4, 12.8, 25.6, and 51.2 μM, respectively) and 20 mM AMP substrate in 36 mM Tris-HCl at pH 7.4 (adjusted at room temperature). The reaction mixtures were incubated at 65 or 85°C for 3 h, and then the samples were treated as described above. Assays with different substrate concentrations were performed using 12 μM wild-type SiRe_0427 protein and increasing concentrations of AMP (5, 10, 20, 30, 40, and 50 mM) in 20-μl reaction mixtures consisting of 36 mM Tris-HCl at pH 7.4 (adjusted at room temperature). The reaction mixtures were incubated at 65°C for 3 h after the reaction was stopped by heating at 98°C for 5 min. The samples were subsequently cooled at 4°C on ice, and then 1 to 2 μl was dotted onto a TLC sheet (Merck Millipore) and separated in a TLC chamber using 1 M NaCl as the mobile phase. Finally, samples were air dried, and the substrate and product were detected using UV lamps at 254 nm.

Effect of temperatures on phosphoribohydrolase activity. The phosphoribohydrolase activity of the wild-type SiRe_0427 protein at different temperatures was examined in a 20-μl reaction mixture containing 6.4 μM SiRe_0427 protein, 20 mM AMP, and 36 mM Tris-HCl (pH 7.4, adjusted at room temperature) at temperature gradients of 25, 35, 45, 55, 65, 75, and 85°C, with a reaction time of 3 h. The activity against the AMP substrate was checked using the procedure in the above-described experiment.

Gene knockout. A two-step crossover (MID) for knockout of a single gene in *S. islandicus* was used for gene deletion analysis as described by Deng et al. (31). For genotype verification of the Δ*sire_0427* strain, the genomic DNA from Δ*sire_0427* was extracted. About 200 ng was used to prepare 25-μl PCR mixtures. The primers used for the plasmid construction and verification are listed in Table 1.

Growth curves. To assess the growth of the wild-type *S. islandicus* REY15A (E233S) and Δ*sie_0427* strains, cells were activated in MCSVU medium. Three parallel cultures of 50 ml were inoculated for each strain, and the OD_{600} was measured after every 6 or 12 h for a period of 3 days. The growth curves were obtained from at least three independent measurements for each sample.

Sensitivity of the Δ*sire_0427* strain to UV irradiation. The effects of UV irradiation on growth of the wild-type and Δ*sire_0427* strain were analyzed by spot assay. About 10 μl of the culture at an OD_{600} of 0.2 was serially diluted (10^0, 10^{-1}, 10^{-2}, 10^{-3}, 10^{-4}, and 10^{-5}) and then dropped onto MCSVU plates. The plates were subsequently exposed to different UV irradiation dosages of 10, 20, and 30 J/m^2 using UV cross-linker (CL-1000 Ultraviolet Cross-Linker; UVP). Finally, the plates were incubated in the dark at 75°C for 7 to 10 days, and the growth of the wild-type and Δ*sire_0427* strains was compared.

SUPPLEMENTAL MATERIAL

Supplemental material for this article may be found at https://doi.org/10.1128/AEM.01739-19.

SUPPLEMENTAL FILE 1, PDF file, 5.5 MB.

ACKNOWLEDGMENTS

We thank the Chinese Scholarship Council (CSC/MOFCOM), People's Republic of China, for providing a scholarship to J.B.M. We also thank Xiuhua Pang for providing *Corynebacterium glutamicum* CgLOG 13032 genomic DNA.

J.B.M. designed the project, performed the experiments, and analyzed the data. Q.H. helped with the application of the instruments and data analysis. Y.X. assisted in protein purification. Q.Z. assisted in construction of the plasmids. J.B.M. wrote the manuscript. J.N. and Y.S. revised the manuscript.

We declare that we have no conflicts of interests.

This study was supported by the National Natural Science foundation of China (no. 31670061 to Y.S.), Fundamental Research Funds of Shandong University (no. 2018HW015 to Q.H.), and China Scholarship Council (CSC)/MOFCOM (no. 2015MOC296 to J.B.M.).

REFERENCES

1. Woese CR, Fox GE. 1977. Phylogenetic structure of the prokaryotic domain: the primary kingdoms. Proc Natl Acad Sci U S A 74:5088–5090. https://doi.org/10.1073/pnas.74.11.5088.
2. DeLong EF, Pace NR. 2001. Environmental diversity of bacteria and archaea. Syst Biol 50:470–478. https://doi.org/10.1080/10635150118513.
3. Cowie ROM, Maas EW, Ryan KG. 2011. Archaeal diversity revealed in Antarctic sea ice. Antarctic Sci 23:531–536. https://doi.org/10.1017/S0954102011000368.
4. Louca S, Mazel F, Doebeli M, Parfrey LW. 2019. A census-based estimate of Earth's bacterial and archaeal diversity. PLoS Biol 17:e3000106. https://doi.org/10.1371/journal.pbio.3000106.
5. Baker BJ, Comolli LR, Dick GJ, Hauser LJ, Hyatt D, Dill BD, Land ML, Verberkmoes NC, Hettich RL, Banfield JF. 2010. Enigmatic, ultrasmall, uncultivated *Archaea*. Proc Natl Acad Sci U S A 107:8806–8811. https://doi.org/10.1073/pnas.0914470107.
6. Spang A, Caceres EF, Ettema T. 2017. Genomic exploration of the diversity, ecology, and evolution of the archaeal domain of life. Science 357:eaaf3883. https://doi.org/10.1126/science.aaf3883.

7. Egorova K, Antranikian G. 2005. Industrial relevance of thermophilic *Archaea*. Curr Opin Microbiol 8:649–655. https://doi.org/10.1016/j.mib.2005.10.015.
8. Kurakawa T, Ueda N, Maekawa M, Kobayashi K, Kojima M, Nagato Y, Sakakibara H, Kyozuka J. 2007. Direct control of shoot meristem activity by a cytokinin-activating enzyme. Nature 445:652–655. https://doi.org/10.1038/nature05504.
9. Skoog F, Armstrong DJ. 1970. Cytokinins. Annu Rev Plant Physiol 21:359–384. https://doi.org/10.1146/annurev.pp.21.060170.002043.
10. Kuroha T, Tokunaga H, Kojima M, Ueda N, Ishida T, Nagawa S, Fukuda H, Sugimoto K, Sakakibara H. 2009. Functional analyses of LONELY GUY cytokinin-activating enzymes reveal the importance of the direct activation pathway in *Arabidopsis*. Plant Cell 21:3152–3169. https://doi.org/10.1105/tpc.109.068676.
11. Tokunaga H, Kojima M, Kuroha T, Ishida T, Sugimoto K, Kiba T, Sakakibara H. 2012. Arabidopsis lonely guy (LOG) multiple mutants reveal a central role of the LOG-dependent pathway in cytokinin activation. Plant J 69:355–365. https://doi.org/10.1111/j.1365-313X.2011.04795.x.
12. Sakakibara H. 2006. Cytokinins: activity, biosynthesis, and translocation. Annu Rev Plant Biol 57:431–449. https://doi.org/10.1146/annurev.arplant.57.032905.105231.
13. Werner T, Kollmer I, Bartrina I, Holst K, Schmulling T. 2006. New insights into the biology of cytokinin degradation. Plant Biol 8:371–381. https://doi.org/10.1055/s-2006-923928.
14. Galuszka P, Spíchal L, Kopečný D, Tarkowski P, Frébortová J, Šebela M, Frébort I. 2008. Metabolism of plant hormones cytokinins and their function in signaling, cell differentiation, and plant development, p 203–264. *In* Attaur R (ed), Studies in natural products chemistry, vol 34. Elsevier, New York, NY.
15. Werner T, Schmülling T. 2009. Cytokinin action in plant development. Curr Opin Plant Biol 12:527–538. https://doi.org/10.1016/j.pbi.2009.07.002.
16. Mok DW, Mok MC. 2001. Cytokinin metabolism and action. Annu Rev Plant Physiol Plant Mol Biol 52:89–118. https://doi.org/10.1146/annurev.arplant.52.1.89.
17. Kukimoto-Niino M, Murayama K, Kato-Murayama M, Idaka M, Bessho Y, Tatsuguchi A, Ushikoshi-Nakayama R, Terada T, Kuramitsu S, Shirouzu M, Yokoyama S. 2004. Crystal structures of possible lysine decarboxylases from *Thermus thermophilus* HB8. Protein Sci 13:3038–3042. https://doi.org/10.1110/ps.041012404.
18. Bae Jeon W, Allard S, Bingman C, Bitto E, Han BW, Wesenberg GE, Phillips G. 2006. X-ray crystal structures of the conserved hypothetical proteins from *Arabidopsis thaliana* gene loci At5g11950 and AT2g37210. Proteins 65:1051–1054. https://doi.org/10.1002/prot.21166.
19. Radhika V, Ueda N, Tsuboi Y, Kojima M, Kikuchi J, Kudo T, Sakakibara H. 2015. Methylated cytokinins from the phytopathogen *Rhodococcus fascians* mimic plant hormone activity. Plant Physiol 169:1118–1126. https://doi.org/10.1104/pp.15.00787.
20. Hinsch J, Vrabka J, Oeser B, Novak O, Galuszka P, Tudzynski P. 2015. *De novo* biosynthesis of cytokinins in the biotrophic fungus *Claviceps purpurea*. Environ Microbiol 17:2935–2951. https://doi.org/10.1111/1462-2920.12838.
21. Samanovic MI, Tu S, Novak O, Iyer LM, McAllister FE, Aravind L, Gygi SP, Hubbard SR, Strnad M, Darwin KH. 2015. Proteasomal control of cytokinin synthesis protects *Mycobacterium tuberculosis* against nitric oxide. Mol Cell 57:984–994. https://doi.org/10.1016/j.molcel.2015.01.024.
22. Burroughs AM, Zhang D, Schaffer DE, Iyer LM, Aravind L. 2015. Comparative genomic analyses reveal a vast, novel network of nucleotide-centric systems in biological conflicts, immunity, and signaling. Nucleic Acids Res 43:10633–10654. https://doi.org/10.1093/nar/gkv1267.
23. Wang W, Ding J, Zhang Y, Hu Y, Wang DC. 2014. Structural insights into the unique single-stranded DNA-binding mode of *Helicobacter pylori* DprA. Nucleic Acids Res 42:3478–3491. https://doi.org/10.1093/nar/gkt1334.
24. Dwivedi G, Sharma E, Rao D. 2013. *Helicobacter pylori* DprA alleviates restriction barrier for incoming DNA. Nucleic Acids Res 41:3274–3288. https://doi.org/10.1093/nar/gkt024.
25. Brimacombe CA, Ding H, Beatty JT. 2014. *Rhodobacter capsulatus* DprA is essential for RecA-mediated gene transfer agent (RcGTA) recipient capability regulated by quorum-sensing and the CtrA response regulator. Mol Microbiol 92:1260–1278. https://doi.org/10.1111/mmi.12628.
26. Mortier-Barriere I, Velten M, Dupaigne P, Mirouze N, Pietrement O, McGovern S, Fichant G, Martin B, Noirot P, Le Cam E, Polard P, Claverys JP. 2007. A key presynaptic role in transformation for a widespread bacterial protein: DprA conveys incoming ssDNA to RecA. Cell 130:824–836. https://doi.org/10.1016/j.cell.2007.07.038.
27. Hovland E, Beyene GT, Frye SA, Homberset H, Balasingham SV, Gómez-Muñoz M, Derrick JP, Tønjum T, Ambur OH. 2017. DprA from *Neisseria meningitidis*: properties and role in natural competence for transformation. Microbiology 163:1016–1029. https://doi.org/10.1099/mic.0.000489.
28. Seo H, Kim S, Sagong H-Y, Son HF, Jin KS, Kim I-K, Kim K-J. 2016. Structural basis for cytokinin production by LOG from *Corynebacterium glutamicum*. Sci Rep 6:31390. https://doi.org/10.1038/srep31390.
29. Seo H, Kim KJ. 2017. Structural basis for a novel type of cytokinin-activating protein. Sci Rep 7:45985. https://doi.org/10.1038/srep45985.
30. Seo H, Kim K-J. 2018. Structural insight into molecular mechanism of cytokinin activating protein from *Pseudomonas aeruginosa* PAO1. Environ Microbiol 20:3214–3223. https://doi.org/10.1111/1462-2920.14287.
31. Deng L, Zhu H, Chen Z, Liang YX, She Q. 2009. Unmarked gene deletion and host-vector system for the hyperthermophilic crenarchaeon *Sulfolobus islandicus*. Extremophiles 13:735–746. https://doi.org/10.1007/s00792-009-0254-2.
32. Athukoralage JS, Rouillon C, Graham S, Gruschow S, White MF. 2018. Ring nucleases deactivate type III CRISPR ribonucleases by degrading cyclic oligoadenylate. Nature 562:277–280. https://doi.org/10.1038/s41586-018-0557-5.
33. Braun F, Thomalla L, van der Does C, Quax TEF. 2019. Cyclic nucleotides in archaea: cyclic di-AMP in the archaeon *Haloferax volcanii* and its putative role. Microbiologyopen 18:e829. https://doi.org/10.1002/mbo3.829.
34. Sayers EW, Barrett T, Benson DA, Bolton E, Bryant SH, Canese K, Chetvernin V, Church DM, Dicuccio M, Federhen S, Feolo M, Fingerman IM, Geer LY, Helmberg W, Kapustin Y, Krasnov S, Landsman D, Lipman DJ, Lu Z, Madden TL, Madej T, Maglott DR, Marchler-Bauer A, Miller V, Karsch-Mizrachi I, Ostell J, Panchenko A, Phan L, Pruitt KD, Schuler GD, Sequeira E, Sherry ST, Shumway M, Sirotkin K, Slotta D, Souvorov A, Starchenko G, Tatusova TA, Wagner L, Wang Y, Wilbur WJ, Yaschenko E, Ye J. 2012. Database resources of the National Center for Biotechnology Information. Nucleic Acids Res 40:D13–D25. https://doi.org/10.1093/nar/gkr1184.
35. Altschul SF, Madden TL, Schäffer AA, Zhang J, Zhang Z, Miller W, Lipman DJ. 1997. Gapped BLAST and PSI-BLAST: a new generation of protein database search programs. Nucleic Acids Res 25:3389–3402. https://doi.org/10.1093/nar/25.17.3389.
36. Edgar RC. 2004. MUSCLE: multiple sequence alignment with high accuracy and high throughput. Nucleic Acids Res 32:1792–1797. https://doi.org/10.1093/nar/gkh340.
37. Larkin MA, Blackshields G, Brown NP, Chenna R, McGettigan PA, McWilliam H, Valentin F, Wallace IM, Wilm A, Lopez R, Thompson JD, Gibson TJ, Higgins DG. 2007. Clustal W and Clustal X version 2.0. Bioinformatics 23:2947–2948. https://doi.org/10.1093/bioinformatics/btm404.
38. Kelley LA, Sternberg MJ. 2009. Protein structure prediction on the Web: a case study using the Phyre server. Nat Protoc 4:363–371. https://doi.org/10.1038/nprot.2009.2.
39. Kumar S, Stecher G, Li M, Knyaz C, Tamura K. 2018. MEGA X: molecular evolutionary genetics analysis across computing platforms. Mol Biol Evol 35:1547–1549. https://doi.org/10.1093/molbev/msy096.
40. Jones DT, Taylor WR, Thornton JM. 1992. The rapid generation of mutation data matrices from protein sequences. Comput Appl Biosci 8:275–282.
41. Contursi P, Jensen S, Aucelli T, Rossi M, Bartolucci S, She Q. 2006. Characterization of the *Sulfolobus* host-SSV2 virus interaction. Extremophiles 10:615–627. https://doi.org/10.1007/s00792-006-0017-2.
42. Sharma R, Rao DN. 2012. Functional characterization of UvrD helicases from *Haemophilus influenzae* and *Helicobacter pylori*. FEBS J 279:2134–2155. https://doi.org/10.1111/j.1742-4658.2012.08599.x.
43. Dwivedi GR, Srikanth KD, Anand P, Naikoo J, Srilatha NS, Rao DN. 2015. Insights into the functional roles of N-terminal and C-terminal domains of *Helicobacter pylori* DprA. PLoS One 10:e0131116. https://doi.org/10.1371/journal.pone.0131116.